Impact behaviour of typical marine composite laminates

L. S. Sutherland and C. Guedes Soares

Abstract

The impact response of five marine laminates has been investigated experimentally and described in terms of undelaminated, delaminated and fibre damage responses. The exact behaviour depended on the thickness to diameter ratio, but at incident energies up to fibre damage the impact responses were very similar for all lay-ups. Fibre damage was most severe for CSM and CSM/WR laminates. The WR and Kevlar/WR laminates were most resilient to fibre damage, but the Kevlar/WR did not perform better than the WR laminate. Energy absorption mechanisms other than damage were thought to be dominant until fibre damage occurs. Inertial interaction effects were more significant than expected.

Keywords

A. Aramid fibre, A. Glass fibres, A. Thermosetting resin, B. Impact behaviour, E. Lay-up (manual)

1. Introduction

The use of laminated composite materials in marine engineering gives the advantages of ease of manufacture of complex forms, resistance to rot, corrosion and chemical attack, high specific mechanical properties and low maintenance. Hence, composites are extensively used for fishing, naval and coastguard vessels and are the material of choice in the leisure boat industry.

However, these composites are susceptible to impact damage, especially out of plane impact. Not only are the more obvious, potentially terminal operational impacts such as collisions with other craft or floating debris and grounding of importance, but relatively minor, everyday impact events such as during docking or objects dropped onto decks or inside the hull may damage the laminate.

Impact damage may be dangerous not only because a breach may lead directly to a loss of the structure at sea, but also because less severe damage may leave the structure unable to support a future unusual load that would be normally within the design limits. Also, damage may grow with the cyclic loadings ubiquitous in the marine environment possibly eventually leading to a catastrophic failure under normal loading. These points are especially dangerous since, as discussed below, damage may well be internal and remain undetected. Hence, large safety factors are often required to allow for impact events, detracting from the potential weight advantages. Mouritz et al. [1] quote safety factors of up to 10 for marine composite structures subjected to impact loads.

Large margins of safety are also needed because of the complexity of the impact behaviour of composite materials. Complete solutions are available for the behaviour of a centrally impacted an-isotropic plate of varying complexity; the classical plate theory (CPT) assumes shear deformation, rotary inertia and normal strain are negligible; first-order shear deformation theory (FSDT or Mindlin Theory) assumes that the transverse shear strains are constant through the thickness but that the transverse normal strain is negligible; higher-

order plate theories (HOPT) assumes that the transverse shear strains and the transverse normal strain have parabolic and linear variations through the thickness, respectively [2].

However, these already non-trivial solutions do not allow for the membrane effects for the higher deflections seen when marine laminates are subjected to impact. Also, they must be solved numerically, lacking the insight into the problem given by analytical methods, and the practical accuracy of such complex methods may be lost due to the difficulties in obtaining accurate experimental material property data.

Further, high local contact forces and the relatively low contact stiffness of the material lead to significant non-linear indentation under the point of impact as investigated in [3]. Hence, the *displacement* (δ) of the impacting object is made up of the sum of the plate *deflection* (w) and the *indentation* (α). A Hertzian contact law [4] fitted well the initial response, but at higher contact loads the response became linear as damage became significant. The transition to linear behaviour was thought to be due to delamination due to complex local contact shear forces.

An alternative approach is to represent the dynamics of the entire system with a spring-mass model [5,6]. This approach is far easier to analyse and to relate to experimental data and is further discussed in Section 4. If the impact event may be assumed to give quasi-static behaviour then an energy balance approach may be taken to give the maximum impact force [5,6]. Here, the incident energy of the impacter is equated to that absorbed by the plate at maximum deflection through bending, shear, membrane and contact deformations.

The greatest complication is, however, that the global plate response is subject in reality to numerous and interacting damage modes including internal delamination, surface micro buckling, fibre fracture and matrix degradation [7]. Previous work [8,9] has shown that the impact response of marine composites may be characterised into three main 'damage regimes':

(i) At very low impact energies the response is close to that of the undamaged plate. Damage is limited to slight permanent indentation and matrix cracking. This was referred to as the 'Un-delaminated' response.
(ii) At a very low incident energy an internal delamination suddenly occurs, with an associated drop in laminate stiffness. This delamination then grows and multiple delaminations at different ply interfaces may occur. This was referred to as the 'Delaminated' response.
(iii) At high incident energies fibre failure occurred, resulting in a drop in or a limiting of the impact force, and leading to perforation or shear failure of the laminate. This was referred to as the 'Fibre Failure' response.

It is important to note that the great majority of the response is dominated by the hidden internal damage, and that visible damage is only seen at much higher incident energies.

These three regimes represent a simplification for characterisation purposes, different impact parameters, such as impacter shape and size, and plate-clamping conditions will give slightly differing responses and damage mechanisms [10]. However, the most important variations seen were between the responses of thin and thick, or more accurately low and high thickness to diameter ratio, laminated plates:

1. Thin plates suffered internal delamination but this was not seen to affect the response significantly. High deflections gave a membrane stiffening effect until at high incident energies back-face fibre failure led to perforation.
2. Thick plates showed both significant shear and indentation deformation. A bi-linear force–displacement response as delamination led to a significant stiffness reduction was seen, followed by front-face initiated fibre failure leading to perforation and/or shear failure.

The exact nature of these damage mechanisms may also be sensitive to even small changes in the many material parameters such as fibre/resin type, ratio, architecture and interface, and laminate production method [11–13]. Further, the most common production method in the marine industry is the hand lay-up of E-glass reinforcement with polyester resin, and hence, material variability adds yet another layer of complexity to the problem.

Hence, given the discussion above it is perhaps not surprising that despite the large amount of work carried out (for example Abrate [2] lists over 500 references, mostly in the aerospace industry concerning expensive high-quality, high volume-fraction, autoclaved, pre-preg carbon-epoxy laminates) the impact response of composite materials is still not well understood. Due to the smaller scale operations of (and hence, much lower finances available to) the marine industry, impact studies of the much lower priced, fibre-content and quality 'marine composites' are extremely rare. Hence, the ranking of these laminates by their impact behaviour is by necessity largely due to experience and reputation, which has unfortunately often been gained in a completely different application.

When a laminate is considered to have 'good impact properties', the complex three-stage impact response explained above has almost certainly not taken into account. It is not enough to say that 'laminate X' performs well under impact, further information as to how well it resists delamination, fibre damage, perforation and how the stiffness is affected by damage and so on should also be considered. It is important to realise that a laminate that performs well in one area may well not perform well in another. It is also worth noting the difference between impact *resistance* (the resistance of the material to impact damage) and impact *tolerance* (how well the material performs once a given impact event has occurred).

Hence, the aim here is to provide measured data for various common marine laminates and then to give an informed and detailed account of how each responds to low-velocity impact taking into account the complexity of the impact event.

2. Experimental details

As common examples of laminates used in marine industry the following laminate schedules were considered; Woven Roving (WR) E-Glass, Chopped-Strand Mat (CSM) E-Glass, combined (alternate) WR/CSM E-Glass, and WR E-Glass with an outer (i.e. next to the mould face) ply of Kevlar 49 (Kevlar/WR). Since, earlier work had suggested that it is the back face of thinner laminates that initiates final fibre failure, a laminate of WR E-Glass with an inner ply of Kevlar 49 (WR/Kevlar) was also considered. This last laminate would also represent a WR laminate with an outer ply of Kevlar impacted from within the structure.

It is important in this study that the impact of each laminate is comparable with that of the other laminates; hence, the respective panels were designed for stiffness equivalence (as far as possible given the discrete numbers of plies) to give equal deflections at equal incident energies (at least for the undamaged case). This is also a pertinent approach since, stiffness

and not strength is usually the limiting factor in most design cases. The reinforcement weights used were 500, 450 and 320 gm^{-2} for WR, CSM and Kevlar, respectively.

In order to investigate both bending and shear controlled behaviour thin and thick laminates of each schedule were considered, respectively. In the case of the Kevlar laminates, the one outer Kevlar ply for the 5-ply laminates was scaled to give three plies for the 15-ply laminates. The laminate schedules are given in Table 1.

'Thin' Panels	**Thickness (mm)**	**'Thick' Panels**	**Thickness (mm)**
$(WR)_5$	3.2 (4.6%)	$(WR)_{15}$	9.3 (3.0%)
$(CSM)_4$	3.6 (7.5%)	$(CSM)_{12}$	10.9 (5.3%)
$(CSM/WR)_2$	3.1 (8.1%)	$(CSM/WR)_6$	9.9 (6.5%)
$(Kevlar)_1\ (WR)_4$	3.2 (5.5%)	$(Kevlar)_3\ (WR)_{12}$	9.0 (3.4%)
$(WR)_4\ (Kevlar)_1$	3.0 (4.6%)	$(WR)_{12}\ (Kevlar)_3$	8.9 (3.5%)

Table 1. Laminate schedules and mean laminate thickness (coefficients of variation in parenthesis)

An orthotropic polyester resin was used throughout to laminate 1 by 1 m panels by hand on horizontal flat moulds. A fibre mass-fraction of 0.5 and 0.3 (equivalent to fibre volume fractions of approximately 0.35 and 0.2) for WR and CSM plies, respectively, was stipulated as representative of the values commonly achieved under production conditions in the marine industry. 1, 2 and 3% by mass of accelerator, catalyst and paraffin, respectively, were used at an ambient temperature of between 18 and 21 °C to cure the resin. 200 mm square specimens were cut from the panels using a diamond-surrounded circular saw. In order to ensure a full cure, all specimens were stored at room temperature for 2 months before testing. Thickness measurements were then taken at four points on each specimen prior to testing.

Impact testing was performed using a fully instrumented Rosand IFW5 falling weight machine. A small, light hemispherical ended cylindrical impacter is dropped from a known, variable height between guide rails onto a clamped horizontally supported plate target. A much larger, variable mass is attached to the impacter and a load cell between the two gives the variation of impact force with time. An optical gate gives the incident velocity, and hence, the impacter displacement and velocity and the energy it imparts are calculated from the force-time data by successive numerical integrations. A pneumatic catching device prevents further rebound impacts. Since, the impacter is assumed to remain in contact with the specimen throughout the impact event, the impacter displacement is used to give the displacement and velocity of the top face of the specimen, under the impacter. By assuming that frictional and heating effects are negligible, the energy imparted by the indenter is that absorbed by the specimen. Thus, this energy value at the end of the test is that irreversibly absorbed by the specimen.

The data may be post-processed with a low pass filter (second-order discrete Butterworth) to remove noise from the signal, and (except for Fig. 10) all data presented here is filtered for clarity. It was found by trial and error that the optimal levels of filtering in order to retain

the pertinent features were 2 kHz for the thin and 4 kHz for the thick laminates, respectively.

The specimens were fully clamped between two thick annular circular steel plates of 100 mm internal diameter. Bolts that passed through the clamp plates and specimen applied the clamping force. Since, most forms are moulded in a female mould and impact generally occurs from the outside, the mould face is the impacted or 'front' face. Tests were carried out using both 10 and 20 mm diameter impactors.

Tests were performed for a range of increasing incident energies either up to perforation where possible, or to the maximum attainable by the machine (210 J). Experience from previous work [9] was used to set the impact masses and incident energy levels (Table 2). Here, the aim was to provide as much data as possible for each of the three damage regimes, and especially around the onsets of internal delamination and fibre-damage.

After testing, the various types of damage were observed and recorded. Since, the material is translucent (and did not have a painted or gel-coated surface as would be the case in practice), the projected internal delamination area could be measured and photographed using strong backlighting.

3. Results

The full results set consists of plots of force, displacement, and absorbed energy against time together with damage photographs (front- and back-face with front- and back-lighting) and damage area and thickness measurements for each of the 160 specimens tested. A summary of these results is presented in this section.

The complex multiple damage modes observed are summarised in Table 2(a) using the coding system given in Table 2(b). Penetration was assumed to have commenced when no rebound occurred. Representative photographs of impact damage are given in Figs. 1–4 where front-face, back-face and back-face with strong backlighting views are shown in (a), (b) and (c), respectively. In order to facilitate cross-referencing of failure modes, the corresponding entries in Table 2(a) have been underlined.

(a)	WR			Kevlar / WR			WR / Kevlar			CSM			CSM / WR		
Nominal IE (J)	IE (J)	Delam. (mm^2)	Fibre Damage	IE (J)	Delam. (mm^2)	Fibre Damage	IE (J)	Delam. (mm^2)	Fibre Damage	IE (J)	Delam. (mm^2)	Fibre Damage	IE (J)	Delam. (mm^2)	Fibre Damage
Thin Laminates, 10mm Diameter Impacter (Impact Mass 3.103kg)															
1	1.3	41a	0	1.3	35a	0	1.1	32a	0	1	0	0	1.1	13#	0
3	3.5	219	0	3.4	197	0	3.1	231	0	3.4	110	0	2.9	138	0
5	5.4	257	0	5.1	260	0	5.1	277	0	5.4	177	0	5.7	334	i#
7	7.5	328	0	7.4	315	0	7.6	391	i#	7.4	257	i#	7.7	396	i#
10	10.2	426	0	9.9	465	0	10.2	421	i/b#	10.4	315	i/b#	10.6	412	i#
15	15.3	448	i#	15.2	517	i#	15.7	559	i/b	15.8	358	f/bSp	15.1	610	i/b
20	20.2	590	i/b#	20.2	736	i/b#	20.7	562	f/bSp	20.2	455	f/bSp	20.2	932	f/bSp
30	30.7	790	f/bSp	30.2	806	f/bSp	30.6	662	f/bSp	30.3	400	p	30.6	1204	p
Thin Laminates, 20mm Diameter Impacter (Impact Mass 3.853kg)															
1	1.3	17#	0	1.1	35a	0	1.5	57a	0	1.4	0	0	1.1	0	0
3	3.1	172	0	3.2	149	0	3.7	202	0	3.4	125	0	3.6	175	0
5	5.3	240	0	5.2	270	0	5.4	303	0	5.4	177	0	5.6	238	0
7	7.8	340	0	7.3	317	0	7.6	446	0	7.5	272	i/b#	7.4	291	i#
15	15.4	517	0	15.2	522	i#	15.8	642	i#/b#	15.2	403	i/b	16	598	i
30	30.1	947	i/b#	30.8	777	i/b#	30.5	780	i/b	30.5	764	f/bSp	30.1	1053	f #/b
50	49.7	1094	f/bSp	49.7	1253	f/bSp	49.7	1041	f/bSp	50.5	904	p	49.7	1417	f/bSp
65	66.6	1196	f/bSp	64.4	1265	f/bSp	65.5	1216	f/bSp	66	936	p	65.5	1836	p
Thick Laminates, 10mm Diameter Impacter (Impact Mass 4.853kg)															
2	2.7	29a	0	2.6	25a	0	1.6	0	0	2.2	0	0	1.5	0	0
5	5.5	152	0	5.3	105	0	6	235	0	5.8	0	0	5.8	105	0
10	10.8	702	i#	10.1	610	i#	10.6	680	i#	11	870	i#	10.7	677	i#
15	15.7	1008	i	15.9	800	i	15.5	975	i	15.2	1106	i	15.2	729	i
30	30.8	1417	f #	30.8	1676	f #	30.8	1881	f #	29.9	1466	f #	29.9	1457	f #
55	55.4	2607	f	55.4	2468	f	55.4	4195	f	54.7	1876	f	55.4	2029	f
75	74.2	2769	f	75.3	3411	f	73.8	3988	f	75.3	2757	f Sp	75.3	3466	f Sp
90	89.7	3743	f	89.7	3915	f	89.7	6086	f	89.7	2782	f Sp	89.7	4824	f Sp
Thick Laminates, 20mm Diameter Impacter (Impact Mass 10.853kg)															
5	5.3	199	0	5.8	145	0	4.7	74	0	6.1	51	0	6.8	100	0
10	12.5	790	0	11.6	618	0	10	568	0	9.7	565	0	10.6	568	0
15	16.8	972	i#	16.1	915	0	14.4	856	i#	15.3	957	i#	15.9	790	i#
30	31	1515	i	30.7	1224	i#	31.8	1921	i	30.7	1524	i	31.5	1148	i
75	75.1	4430	i/+#	76.7	4135	i#+	77.9	6360	i/+	76.7	3245	i	75.1	4377	i/+#
90	91.7	5739	i/+	92.6	5660	i/+	91.7	6231	i/+	90.3	3541	f #	89.4	5209	i/+
150	151	9552	i/+	153	9574	i/+	151	9282	$f^{\#}+b^{\#}$	151	6753	f/b#	150	9529	f/+
210	208	10823	f/+	212	10537	f/+	208	11187	f #/+	212	7515	f/bSp	208	10956	f/+

(b) Coding System

f : Front-face
b : Back-face
i : Indent
: Very slight
Sp : Start of penetration
p : Penetration

Delamination identifiable from force-deflection plot
Fibre damage identifiable from force-time plot
Underlined entries correspond to Figures 1 to 4

Table 2. Observed failure modes (a) and coding system (b)

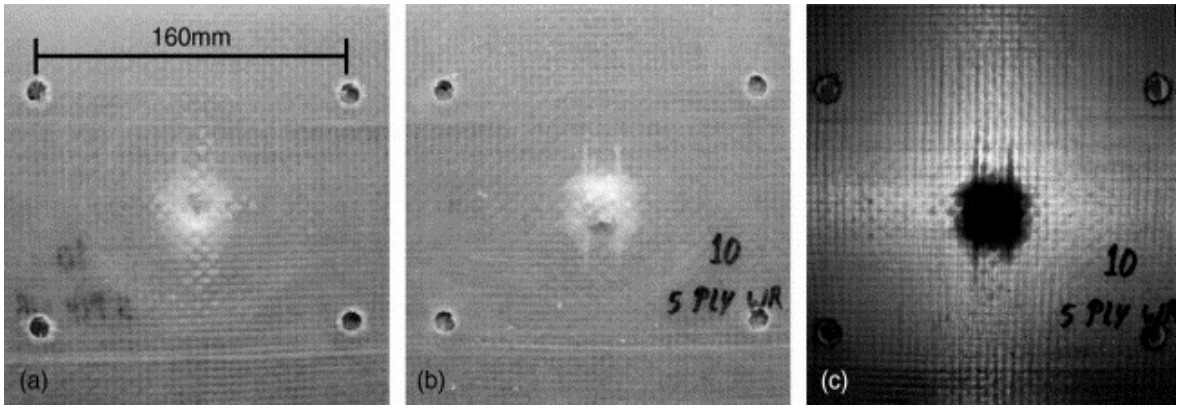

Fig. 1. Typical impact damage, thin WR (20 mm Ø Impactor, 50 J).

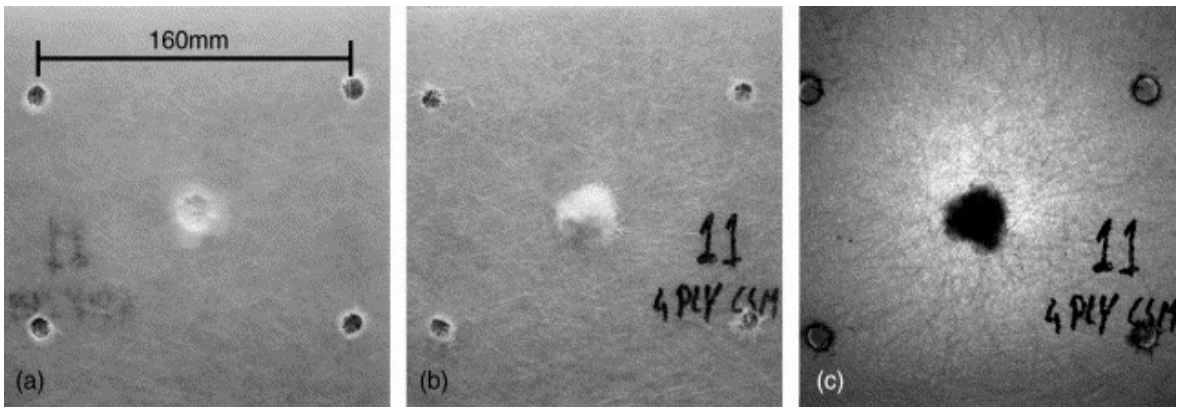

Fig. 2. Typical impact damage, thin CSM (20 mm Ø Impactor, 30 J).

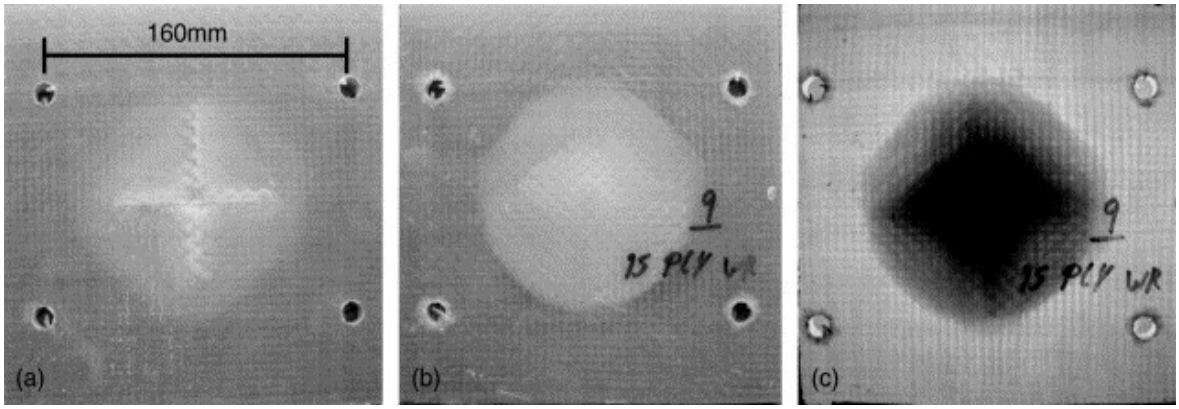

Fig. 3. Typical impact damage, thick WR (20 mm Ø Impactor, 210 J).

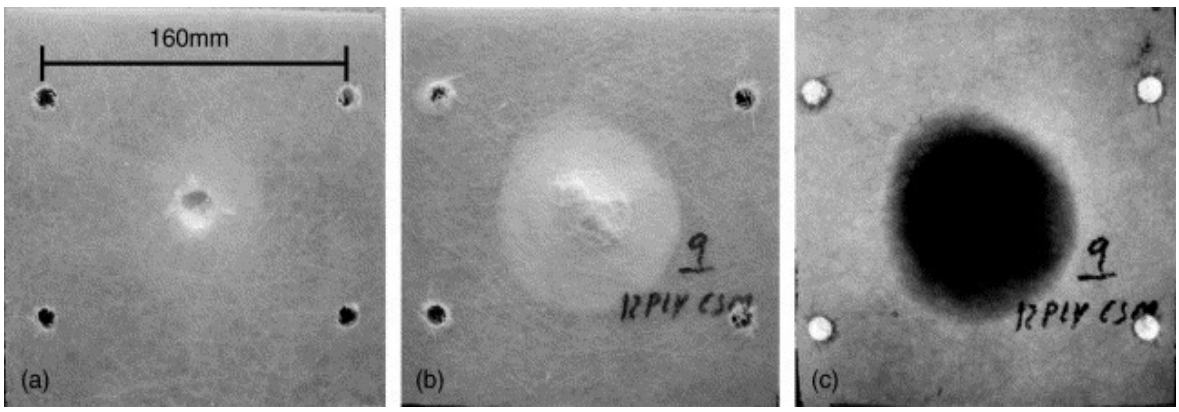

Fig. 4. Typical impact damage, thick CSM (20 mm Ø Impactor, 210 J).

Typical impact responses for thin and thick plates are shown in Fig. 5(a)–(d), respectively. The whole family of tests for increasing incident energy is shown on each plot.

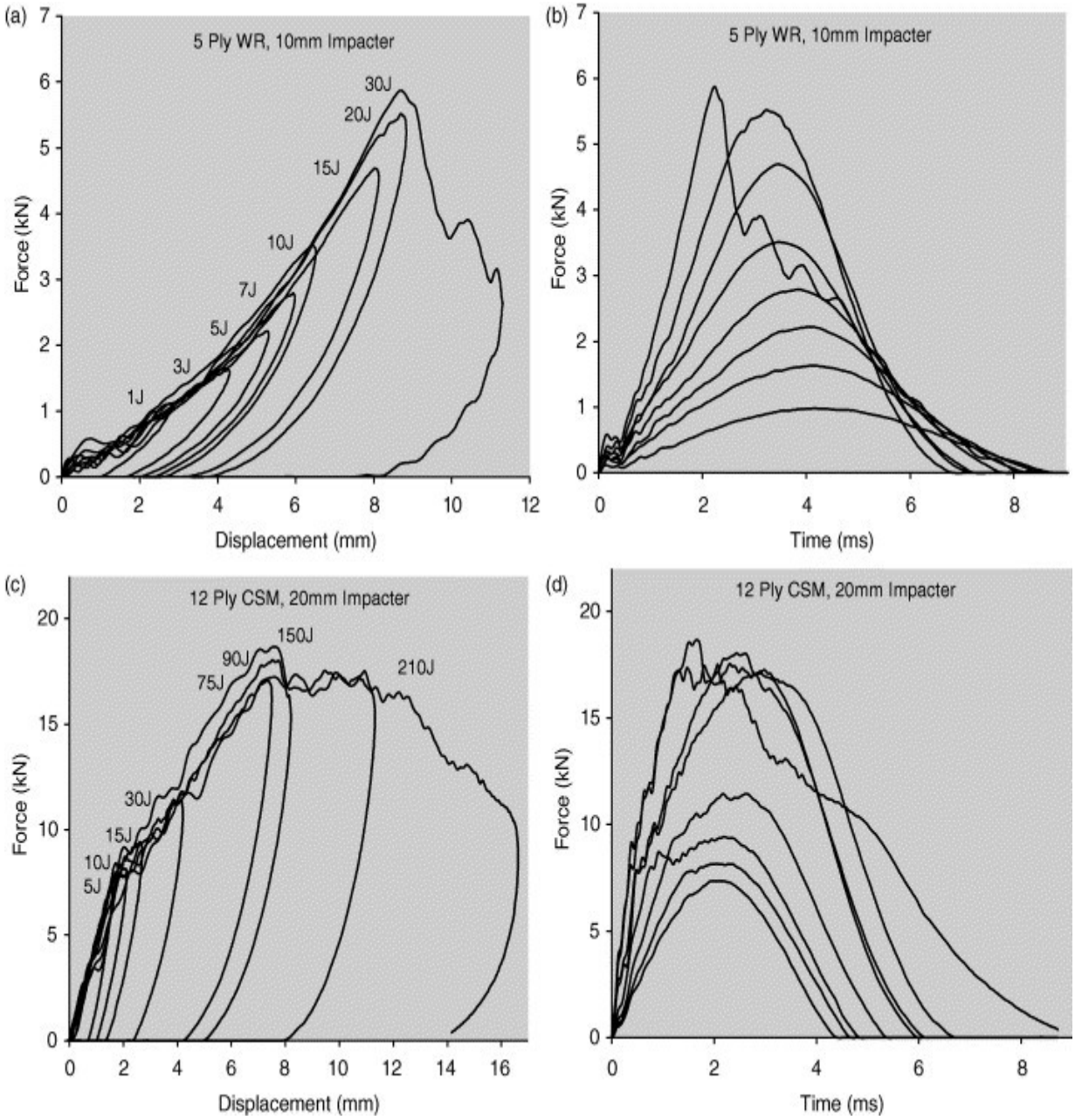

Fig. 5. Typical impact responses of thin (a and b) and thick (c and d) plates.

For thin plates Fig. 5(a) shows the increasing stiffness with displacement because of membrane effects due to the large deflections seen, and this is reflected in the decreasing impact durations indicated in Fig. 5(b). Despite the fact that internal delamination of thin plates was observed (Table 2) this is seen not to affect the impact response. At the highest impact energies, the back-face fibre damage of thin plates (Table 2) is reflected in the response plots, and this causes an increase in the impact duration. However, where permanent indentation damage was observed at slightly lower incident energies than fibre damage (Table 2), this was not indicated in the response plots.

The initial small peak, especially visible in Fig. 5(b), was found to be due to the way in which the low-pass filter used processes initial decaying vibrations in the force signal, and this aspect is fully discussed in Section 4.

In Fig. 5(c) and (d) the three-stage impact behaviour described in the introduction is clear for the thick plates; an initial stiff *undelaminated* response is followed by a less stiff *delaminated* response, and at high incident energies *fibre damage* (in this case on the front-face) leads to a drop in impact force. Impact duration increases as delamination becomes progressively more severe, and then as fibre damage occurs. However, the permanent indentation (and, for the 20 mm diameter impactor, the cross-shaped front-face delamination damage) seen at slightly lower incident energies than fibre damage (Table 2) was not identifiable from these response plots.

The shaded entries in Table 2 show that a drop in stiffness is only visible in the response plots of the thick plates after the delaminated area became greater than approximately 200 mm^2. The initiation of internal delamination is shown in Fig. 6. The small delaminations seen at the lowest incident energies as in Fig. 6(a) and (b) were seen to be close to the front surface, and were thought to be solely due to contact forces. These small 'contact delaminations' were not accompanied by a drop in stiffness in the force–displacement plots. At slightly higher incident energies a larger delamination then occurred deeper within the laminate (Fig. 6(c)), which corresponded to the observed reduction in plate stiffness response.

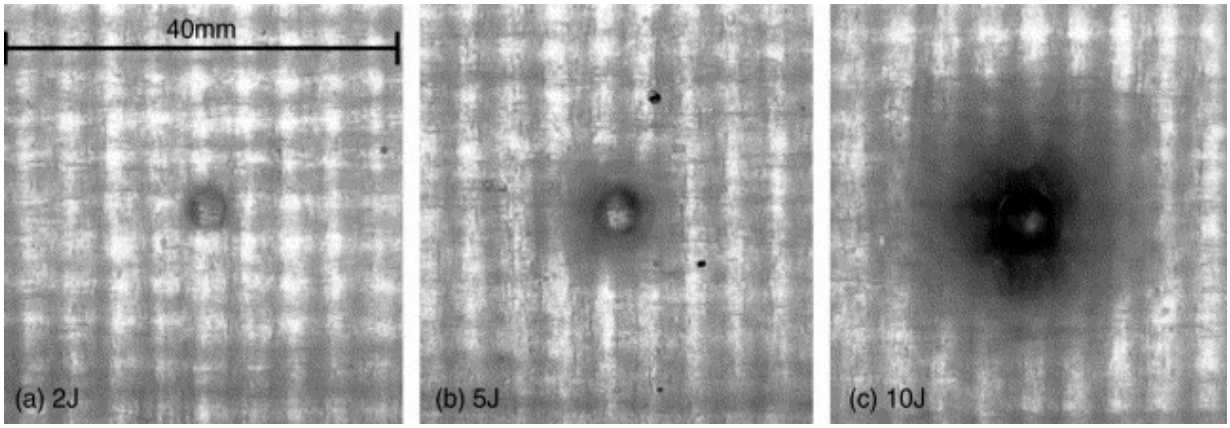

Fig. 6. Initiation of internal delamination (thick WR, 10 mm Ø Impactor).

It is not practical to include the impact response plots of all 160 tests here, but the important trends are summarised below in maximum impact force, absorbed energy and projected damaged area vs. incident energy plots in Figs. 7–9, respectively.

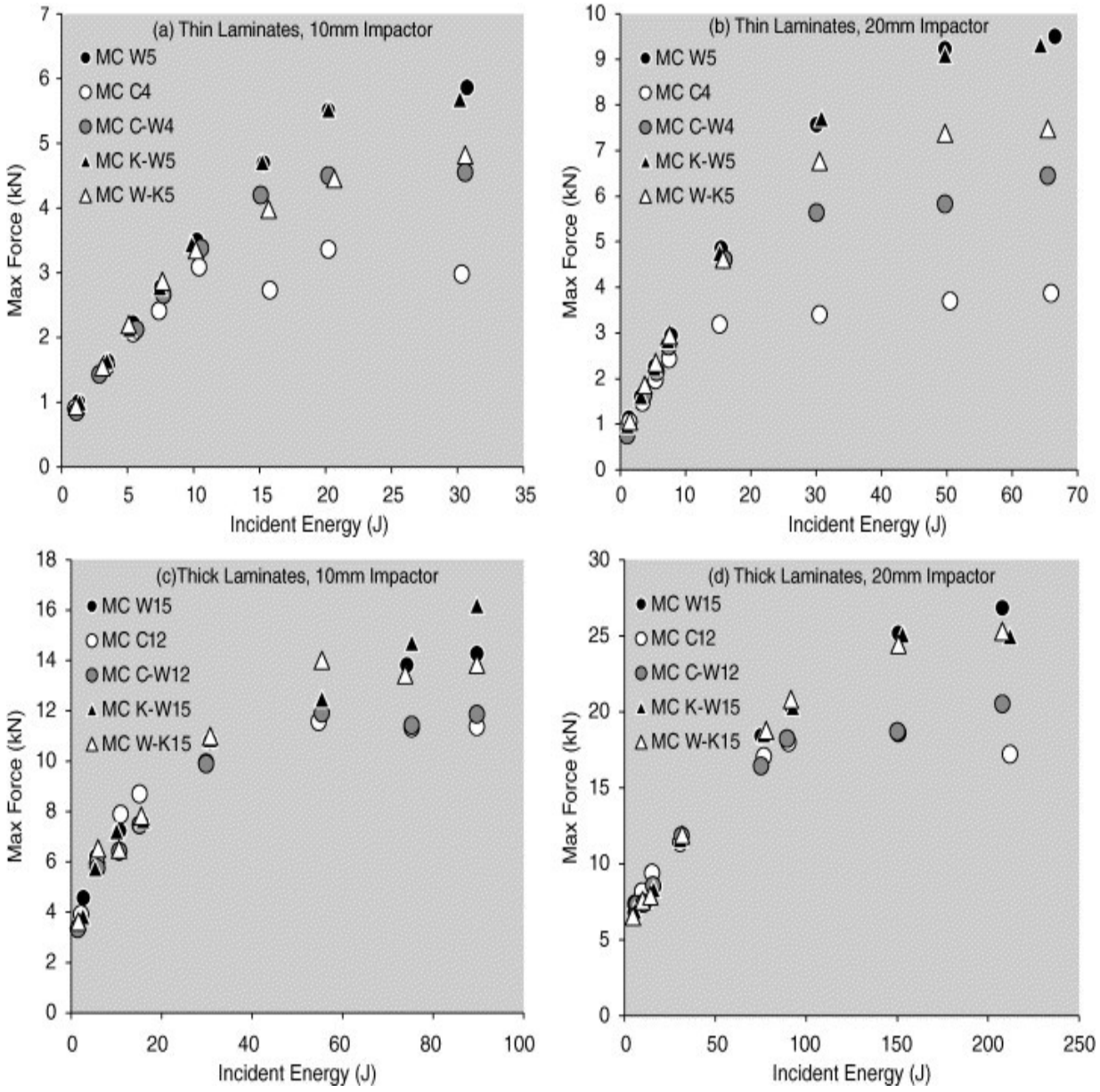

Fig. 7. Maximum force impact response vs. incident energy.

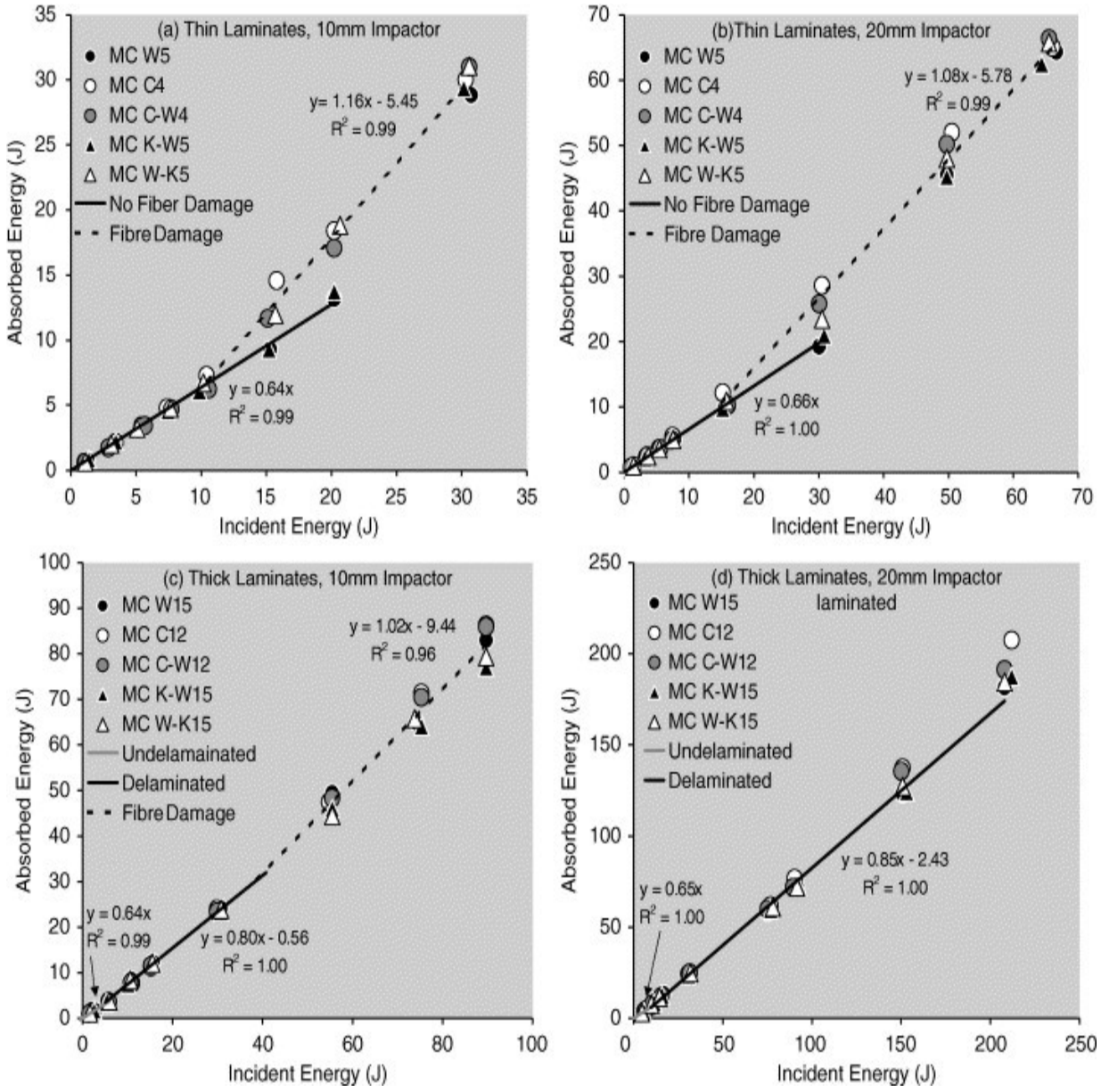

Fig. 8. Irreversibly absorbed energy impact response vs. incident energy.

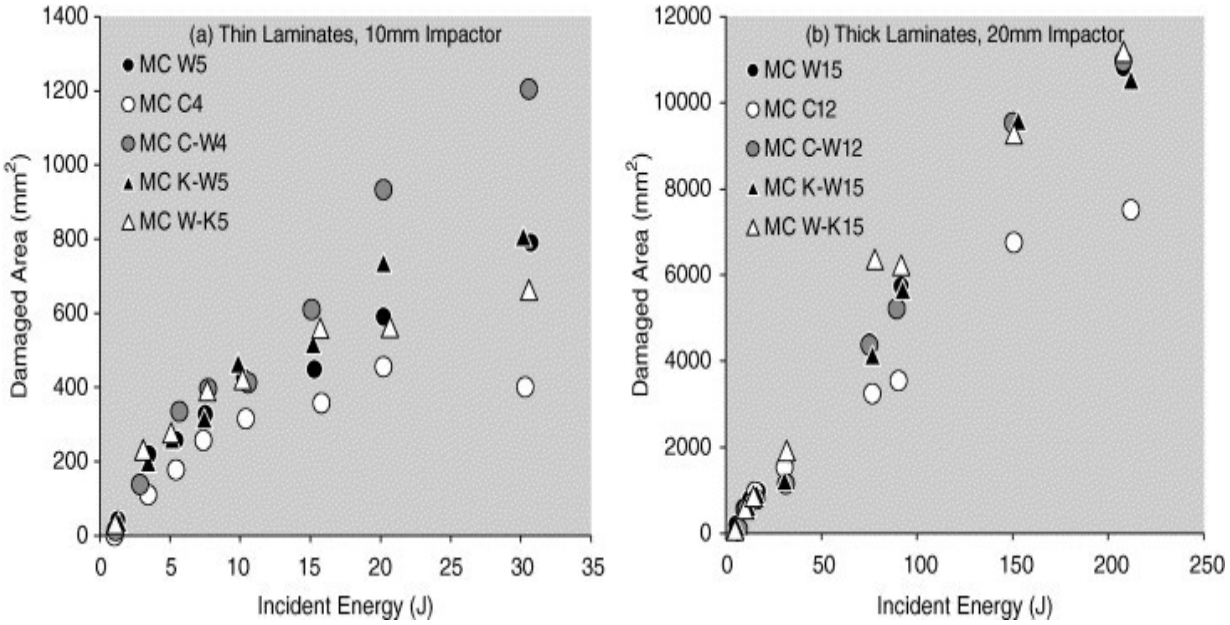

Fig. 9. Projected damaged area impact response vs. incident energy.

4. Analysis and discussion of results

4.1. Inertial interaction between plate and impacter masses

As mentioned in Section 3, an initial peak was often seen in the filtered force–time response (e.g. Fig. 5(b)). Analyses of the unfiltered data showed this to be due to the filtering of a decaying sinusoidal signal, superimposed onto the impact response. As examples of this behaviour, the unfiltered force–displacement responses of the four plate thickness-impactor diameter combinations for an incident energy of 30 J are shown in Fig. 10. The initial 'vibration' in the signal is by far strongest for the thick 10 mm diameter results (Fig. 10(c)).

Shivakumar [5] shows that this type of perturbation occurs due to interacting inertial forces of the plate and impactor masses, which vibrate around the contact stiffness n (Fig. 11) so that the indentation α (i.e. x_1-x_2) has a cyclic variation with time. In Fig. 11, K_b, K_s and K_m are bending, shear and membrane stiffness of the plate, respectively. Shivakumar states that Leissa [14] suggests that the plate mass may be neglected to give a single degree-of-freedom system if the impactor mass is greater than 3.5 times that of the plate, and in this case these perturbations will not be significant. However, these vibrations are very significant in Fig. 10(c) despite the much higher impactor/plate mass ratio (m_1/m_p) of 40.

It is not clear exactly how the value of 3.5 is deduced from reference [14] in Ref. [5], but the indication that the effective mass of the plate contributing to inertial effects is one fourth of its mass appears to have its origins in an approximate study of a simply supported rectangular plate with a point mass at its centre [15]. However, what can be assumed here is that these inertial effects will become more significant not only with an increasing plate to impactor mass ratio, but also with a decreasing contact stiffness. Here, the contact stiffness of the resin-rich marine composites [3] will be much lower than that of the aluminium plate considered by Shivakumar, leading to a greater significance of plate inertial effects.

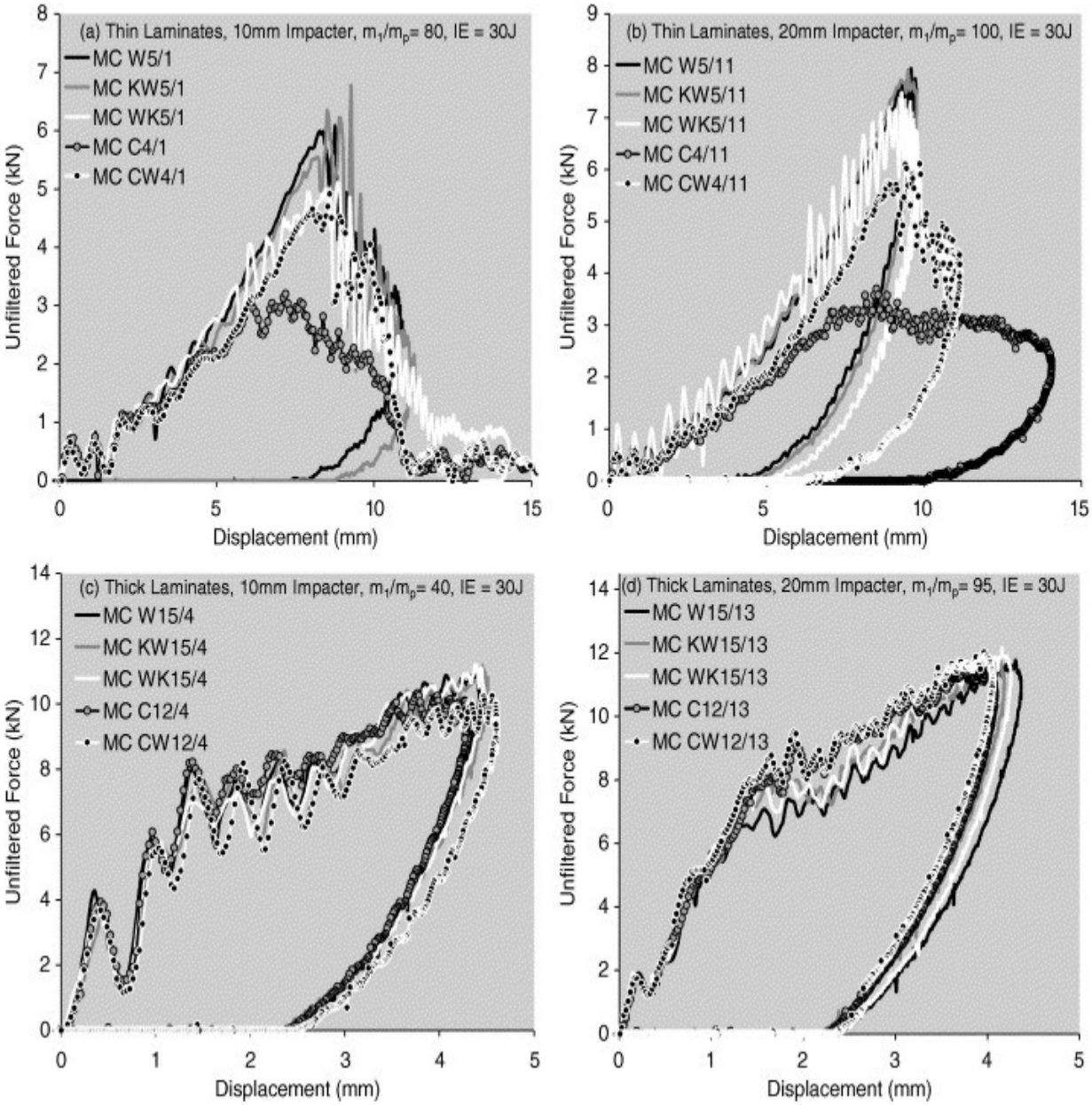

Fig. 10. Unfiltered force vs. displacement plots showing inertial interaction between impact and plate masses (m_1 and m_p, respectively).

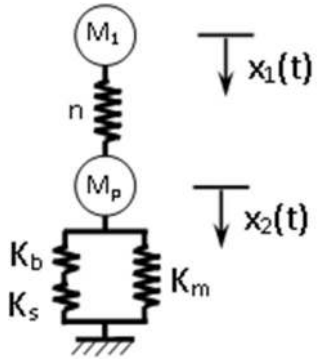

Fig. 11. Two degree-of-freedom spring-mass model of impact event.

Inertial effects are also visible in the unfiltered data for the other tests shown in Fig. 10(a), (c) and (d) where the values of m_1/m_p are even higher, but these quickly attenuate, probably due to the material damping of these resin-rich laminates and/or localised contact damage.

Two anomalous observations reinforce the deduction that these perturbations are in fact due to plate inertial effects. The first is that the thick WR/Kevlar test with the 10 mm diameter impactor at 75 J exhibited more vibration than the equivalent tests on the other four laminates. The impactor mass in this case was only 3.853 kg instead of 4.853 kg since, this was the first test and after the results were analysed it was decided to use the larger mass for all 159 subsequent tests. This gave a value of m_1/m_p of 34 instead of 40 which would give greater inertial interaction and hence, perturbations.

The second is the much higher vibrations for the WK5/11 response seen in Fig. 10(b) than for the other four laminates. It was noticed after this test that the hemispherical end of the impactor head had become slightly loose. The effect of this can be thought of as a drastic reduction in effective contact stiffness, which would again explain the increased perturbations. After the head was re-tightened this effect disappeared.

The above discussion shows that great care must be taken when filtering the data, features that may appear to be only due to noise may in fact part of the system response. Conversely, it would be easy to mistake the peak due to the filtered vibrations here for the characteristic drop in load associated with damage events (e.g. the initial 'peak' in Fig. 10(d)).

5. Impact response of thin laminates

Fig. 12 (together with Table 2) allows comparisons of the progression of damage with increasing incident energy to be made between the five thin laminates. The overall damage sequence is delamination, a slight permanent indent, back-face then front-face damage and finally penetration. It is clear that the WR and Kevlar/WR laminates are the most resistant to fibre damage and exhibit an almost identical response. The WR/Kevlar and CSM laminates are the first to show slight fibre damage. However, the CSM fibre damage quickly becomes much worse and it was these specimens that were first to suffer penetration. WR/Kevlar and CSM/WR suffer the next worse fibre damage and exhibit approximately equivalent responses, but of the two WR/Kevlar resisted penetration slightly better.

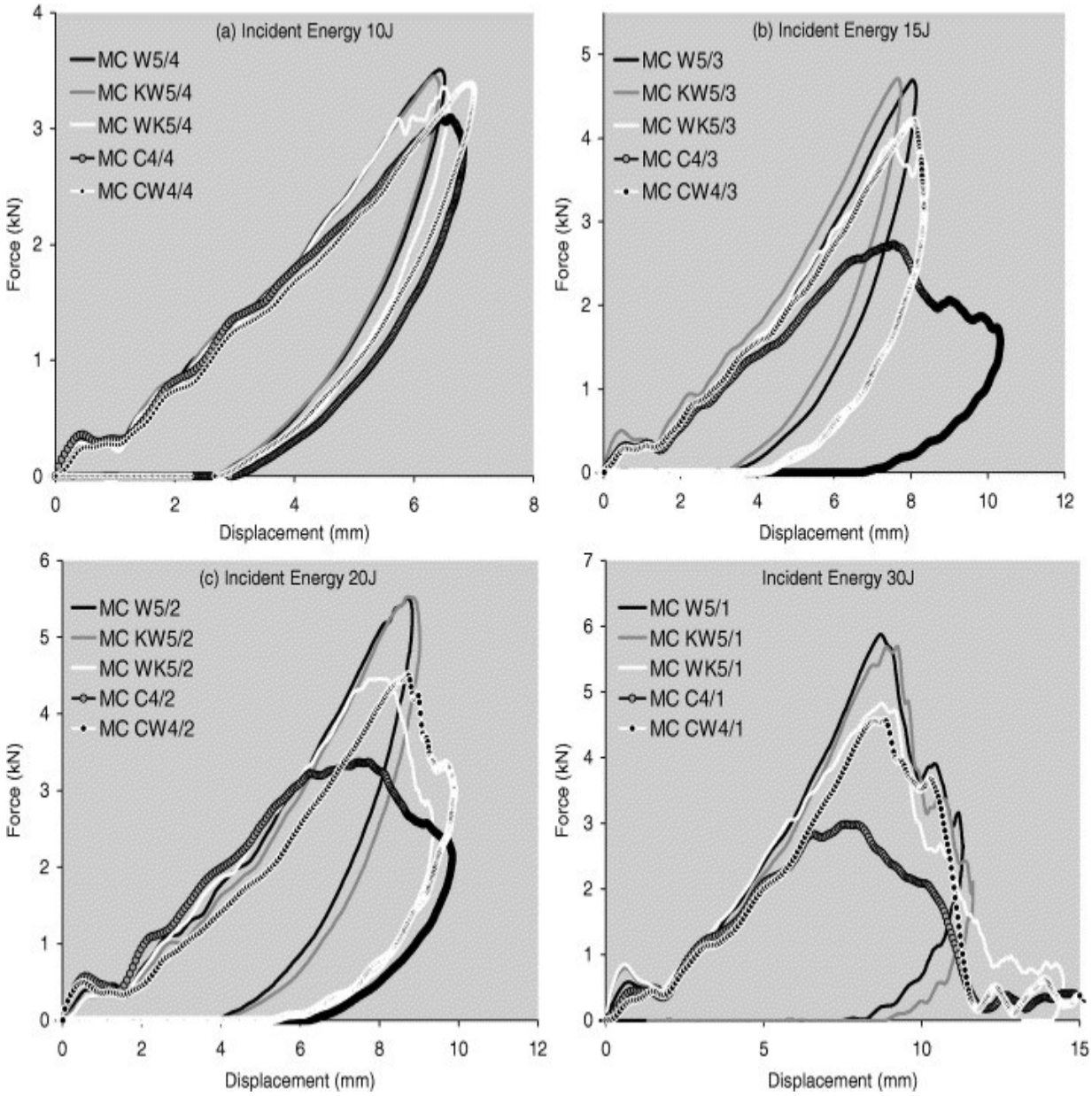

Fig. 12. Thin laminate (impactor diameter 10 mm) force–displacement plots showing typical damage progression.

Very similar maximum displacements were observed for all five laminates, showing that the aim of producing plates of the same stiffness had been achieved. It was only when fibre damage became significant when the CSM/WR and especially the CSM maximum displacements significantly exceeded those of the other thin laminates as penetration occurred.

The maximum impact forces of Fig. 7(a) and (b) are more sensitive to the start of fibre damage than are the maximum displacements, but these values also do not vary between laminates before fibre damage occurs. As expected, the laminates giving the lowest impact forces were those suffering the most damage. The CSM laminates gave the lowest forces, followed by CSM/WR and WR/Kevlar, with the most resistant WR and Kevlar/WR specimens producing the highest impact forces.

The high R^2 values shown in Fig. 8(a) and (b) show that very strong linear trends are present in the relationships between absorbed and incident energies. Sixty-five percent of the incident energy is absorbed irreversibly for the undelaminated response, and this figure remains constant after delamination occurs. This indicates that mechanisms other than delamination are responsible for most of the energy absorption. It is thought that the most probable mechanism for these resin-rich laminates is material damping, but matrix micro cracking and/or other mechanisms may also be contributory and this requires further investigation. Fibre damage is accompanied by a marked increase in the absorbed-incident energy ratio. The ability of the WR and Kevlar/WR laminates to resist fibre damage until higher incident energies is clear from Fig. 8(a) and (b).

Fig. 9 shows that thin specimens suffer much less delamination than thick specimens. Delamination is seen in Fig. 9(a) to occur at approximately the same extremely low incident energy for all five laminates. CSM laminates suffered slightly less delaminated area. The delamination of the other four laminates was approximately equal until after the onset of fibre damage when more scatter occurred, but CSM/WR delamination was severest.

Overall, the responses and damage mechanisms were very similar for both diameters of impactor, but damage occurred at significantly lower incident energies with the 10 mm diameter impactor.

6. Impact Response of thick laminates

Fig. 13 (along with Table 2) enables the damage development with increasing incident energy to be compared between the five thick laminates. The general progression of damage was of delamination then permanent indentation, followed by front-face fibre damage leading to penetration. Additionally, plates containing WR plies (i.e. all except for the CSM plates) struck by the 20 mm diameter impactor also suffered a cross-shaped top ply delamination/buckling (Fig. 3(a)), which occurred at a slightly higher incident energy than did the indentation.

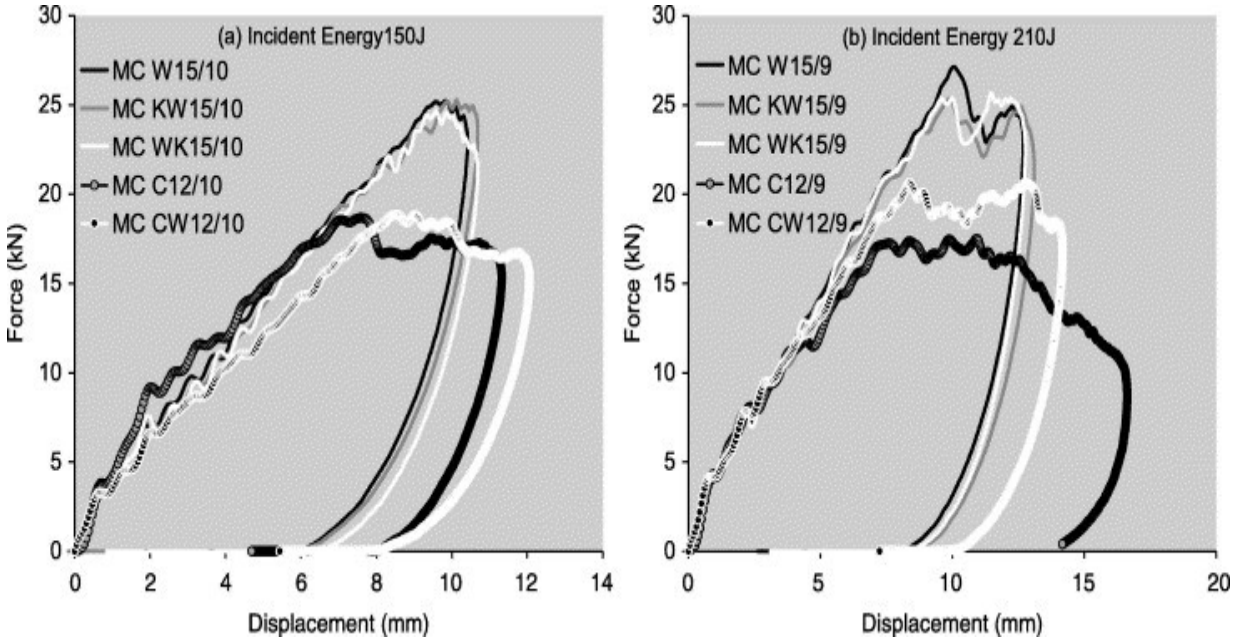

Fig. 13. Thick laminate (impactor diameter 20 mm) force–displacement plots showing typical damage progression.

Both indentation and cross delamination occurred at approximately the same incident energies for all thick laminates. With the 10 mm diameter impactor, front-face fibre damage occurred at approximately the same incident energy for all laminates. However, with the 20 mm diameter impactor, the CSM and CSM/WR laminates were the first to suffer front-face damage. At higher incident energies the fibre damage was most severe for CSM and CSM/WR laminates. At the maximum incident energies used here the start of penetration was only seen for the CSM and WR/CSM laminates with the 10 mm diameter impactor, and for the CSM laminate with the 20 mm diameter impactor.

The five thick laminates were seen to be of equivalent stiffness. As penetration commenced the maximum displacements of the CSM and CSM/WR plates started to exceed those of the other thick laminates.

The maximum impact forces of Fig. 7(c) and (d) also do not vary between laminates before fibre damage occurs. Again, only CSM and WR/CSM maximum forces were limited by the onset of penetration.

The strong linear trends in Fig. 8(c) and (d) show that (as for the thin laminates) 65% of the incident energy is absorbed irreversibly during the tests for the very short undelaminated response of the thick laminates. However, in this case an increase to 80% occurs with delamination. Fibre damage is accompanied by an increase in absorbed-incident energy, but due to the upper energy limit of the test machine this is not fully developed.

Fig. 9(b) shows that delamination occurs at a very similar low incident energy for all five laminates. All laminates suffered similar degrees of delamination until fibre damage occurred, after which CSM delamination was generally smaller, and more scatter was seen in the data.

Damage occurred at significantly lower incident energies with the 10 mm diameter impactor. The only significant difference in behaviour was the cross-shaped top ply delamination/buckling (Fig. 3(a)), which was only produced by the 20 mm diameter impactor.

7. Conclusions

The impact response of five common marine laminates has been investigated through an extensive experimental study, and described in terms of undelaminated, delaminated and fibre damage behaviour.

Thick specimens gave a marked reduction of stiffness as internal delamination occurred, and then front-face fibre damage led to penetration.

The response of thin specimens was mainly membrane controlled until back-face fibre damage led to penetration. Delamination of thin plates occurred, but was much smaller than for the thick specimens, and did not significantly affect the response.

Delamination of all laminates occurred at very low incident energies, which were not dependant on laminate type. A small initial surface delamination occurred (thought to be due to contact forces), followed by a deeper and larger internal delamination due to global plate stresses.

For both thick and thin plates, at incident energies where no fibre damage occurred there was very little effect of laminate lay-up on the impact response.

The impact behaviour seen is summarised in Table 3. The complexity of this behaviour, and its sensitivity to the exact nature of the impact event, shows that the definition of the impact behaviour of a laminate must be correspondingly comprehensive.

	Thin laminates	**Thick laminates**
Undelaminated	65% incident energy irreversibly absorbed	
Delaminated	Started at same IE for all laminates	
	Area≪Thick laminates	Area≫Thin laminates
	Slightly smaller for CSM	
	65% IE irreversibly absorbed	80% IE irreversibly absorbed
Fibre damage	Back-face occurred first WR/K and CSM first to suffer	Front-face occurred first: 10 mm Ø impactor, onset fibre damage independent of laminate; 20 mm Ø impactor, CSM and CSM/WR first to suffer
	Resistance to fibre damage: WR and K/WR>WR/K>CSM/WR≫CSM	Resistance to fibre damage: WR, K/WR and WR/K≫CSM/WR>CSM
	CSM damage generally smaller	CSM damage slightly smaller
	CSM/WR damage largest	

Table 3. Summary of impact behaviour

The laminates of WR and of WR with an outer Kevlar layer were consistently significantly more resilient to fibre damage. However, there was no difference between their, respective, impact responses. Hence, the common practice of substituting a few outer plies of glass with Kevlar does not appear to significantly improve impact response under the conditions studied here (but would increase raw material costs and make cutting, laminating and repair more problematic).

The force–time and force–displacement response plots could be used to identify the onset of internal delamination of thick plates, and of fibre damage of both thin and thick plates. However, the effects of internal delamination of thin plates, indentation of both thin and thick plates, and front-face ‘cross’ creasing delamination of thick plates were not distinguishable from these plots.

Sixty-five percent of the incident energy was absorbed irreversibly even when no significant damage had occurred. Even with significant delamination of the thicker specimens this only rose to 80%. Hence, energy absorption mechanisms other than damage are thought to be dominant until fibre damage occurs.

Inertial interaction effects were significant for much lighter plates than quoted in the literature. This was thought to be due to the low contact stiffness of marine composites.

Acknowledgements

This work has been performed within the project 'MARSTRUCT—Network of Excellence on Marine Structures' (http://www.mar.ist.utl.pt/marstruct/) and has been partially funded by the European Union through the Growth programme under contract TNE3-CT-2003-506141.

References

[1] Mouritz AP, Gellert E, Burchill P and Challis K. Review of advanced composite structures for naval ships and submarines. Composite Structures 2001;53:21-41.

[2] Abrate S. Impact on Composite Structures. Cambridge University Press, Cambridge UK, 1998.

[3] Sutherland LS. and Guedes Soares C. Contact Indentation of Marine Composites, Composites Structures 2004; in press: available online.

[4] Johnson KL. Contact Mechanics. Cambridge University Press, Cambridge UK, 1985.

[5] Shivakumar KN., Elber W. and Illg W. Prediction of impact force and duration due to low-velocity impact on circular composite laminates. J Appl Mech 1985;52:674-680.

[6] Abrate S. Modelling of impacts on composite structures. Composite Structures 2001; 51:129-138.

[7] Richardson MOW. and Wisheart MJ. Review of low-velocity impact properties of composite materials. Composites: Part A 1996;27A:1123-1131.

[8] Sutherland LS. and Guedes Soares C. Effects of laminate thickness and reinforcement type on the impact behaviour of e-glass/polyester laminates. Composites Science and Technology 1999;59:2243-2260.

[9] Sutherland LS. and Guedes Soares C. Impact characterisation of low fibre-volume glass reinforced polyester circular laminated plates. Int J Impact Eng 2005;31:1-23.

[10] Sutherland LS. and Guedes Soares C. The effects of test parameters on the impact response of glass reinforced plastic using an experimental design approach. Composites Science and Technology 2003;63:1-18.

[11] Cartié DDR. and Irving PE. Effect of resin and fibre properties on impact and compression after impact performance of CFRP. Composites: Part A 2002;33:483-493.

[12] Caprino G. and Lopresto V. On the penetration energy for fibre-reinforced plastics under low-velocity impact conditions. Composites Science and Technology 2001;61:65-73.

[13] Hirei Y., Hamada H. and Kim JK. Impact response of woven glass-fabric composites – I. Effect of fibre surface treatment. Composites Science and Technology 1998;58:91-104.

[14] Leissa AW. Vibrations of Plates. NASA SP-160, 1969.

[15] Wah, T. Natural frequencies of plate-mass systems, Proc Indian Soc Theor and Appl Mech 1961:157-168.